Progress In Electromagnetics Research Letters, Vol. 99, 83–91, 2021

A Compact Dual-Band Flexible Antenna for Applications at 900 and 2450 MHz

Adnan Ghaffar[1, *], Wahaj A. Awan[2], Niamat Hussain[3], Sarosh Ahmad[4], and Xue Jun Li[1]

Abstract—A dual band flexible antenna for applications at 900 and 2450 MHz is proposed in this paper. The antenna offers a compact size of $0.23\lambda_o \times 0.120\lambda_o \times 0.0007\lambda_o$, where λ_o is the wavelength at the lower resonance. The antenna comprises a simple geometrical structure consisting of a W-shaped serpentine structure fed by a microstrip line, while a Defected Ground Structure (DGS) technique was utilized with a partial ground plane to achieve wide operational bandwidth. An additional capacitor was loaded in between the slots to achieve a higher resonance, thus resulting in a compact dual-band antenna. Various performance parameters were analyzed, and results were compared with the measured ones. The antenna offers good performance in terms of size, bandwidth, gain, and radiation pattern and thus increases the potential of the proposed antenna for both rigid and flexible devices.

1. INTRODUCTION

Industrial, Medical and Scientific (ISM) frequency band is one of the most used bands. Several technologies adopted this band to operate, including but not limited to cordless phones, Near Field Communication (NFC), Bluetooth, and Wi-Fi [1, 2]. Besides these, it finds its application in the medical field as well. For instant, hyperthermia therapy uses 2.45 GHz ISM band frequency to cure cancer [3]. Moreover, this band is also used in industries for induction heating, softening plastic, welding of plastic, and microwave heat treating [4]. Thus, this band becomes the most important frequency band in our daily life.

In the modern era, the usage of flexible/semi-flexible devices increases exponentially due to their numerous advantages over rigid devices, and these advantages include durability, light weight, flexibility, portability, and good energy efficiency [5, 6]. Antenna, being a key component of any communication system for its responsibility of transmitting and receiving a signal, plays a major role in designing a compact communication system [7]. Moreover, for a flexible device, a huge demand for flexible antennas arises. Thus, researchers are trying to design optimal antennas. Various performance parameters have been considered by the researchers including overall size, wide bandwidth, high gain, and low-level complexity of antenna along with obtaining matching results for both conformal and non-conformal conditions.

Researchers have designed several single and dual band flexible antennas for 900 MHz and 2450 MHz, which are the most commonly used ISM bands [8–19]. For instance, a compact flexible fractal antenna was presented in [8] at 2450 MHz. Although the reported work had advantages like wide bandwidth, compact size, and high gain, it did not propose any solution for 900 MHz. A dual-band flexible antenna having a dimension of 100 mm × 60 mm was presented in [9], which had dual-band operation with a

Received 6 June 2021, Accepted 23 July 2021, Scheduled 3 August 2021

* Corresponding author: Adnan Ghaffar (aghaffar@aut.ac.nz).
[1] Department of Electrical and Electronic Engineering, Auckland University of Technology, Auckland 1010, New Zealand.
[2] Department of Integrated IT Engineering, Seoul National University of Science and Technology, Seoul 01811, South Korea.
[3] Department of Information and Communication Engineering, Chungbuk National University, Cheongjou 28644, South Korea.
[4] Department of Electrical Engineering and Technology, Government College University Faisalabad (GCUF), Pakistan.

wide bandwidth, but its performance was adversely affected by bending, limiting its applications to rigid circuits. A miniaturized dual-band antenna for ISM band applications was proposed in [11]; however, it had drawbacks like rigid structure and narrow bandwidths. Another compact antenna was presented in [12], where varactors tuning was utilized to shift the frequency from 2.45 GHz to 900 MHz; however, this work also suffered from the rigid structure and narrow bandwidth at both resonances.

In [14], a tri-band antenna was presented for 900, 1800, and 2450 MHz band applications. The antenna consisted of a simple geometrical structure along with a compact size of 43.5 mm × 48 mm. However, the antenna suffered from a rigid structure, narrow bandwidth, and low gain. Next, a paper substrate-based dual-band flexible antenna was presented in [15]. The antenna offered wide operational bandwidth with drawbacks such as large dimension and negative gain at lower resonance. Contrary to this, a dual-band flexible antenna based on the felt substrate was presented in [16], which offered compact size along with reasonable gain at the cost of structural complexity due to vias and unsatisfactory performance in the conformable condition.

Thus, it can be deduced from the aforementioned analysis that there is still a need for a compact flexible antenna with wide operational bandwidth, simple geometrical structure, and high gain. Therefore, a dual-band flexible antenna is presented in this paper with the following key features:

- To the best of the authors' knowledge, it is the most compact flexible antenna among the reported works in the literature.
- The proposed antenna offers wide bandwidth at 900 MHz and 2450 MHz along with reasonable gains.
- The antenna achieves good agreement between simulated and measured results in both bent and unbent conditions, thus making the proposed antenna a promising candidate for both conformal and non-conformable devices.

2. ANTENNA DESIGN AND METHODOLOGY

2.1. Antenna Design

Figure 1 illustrates the geometrical configuration of the proposed dual-band flexible antenna. The antenna was designed utilizing the flexible material by ROOGERS Corp., RT-5880 with relative permittivity (ε_r) of 2.2 and loss tangent (tanδ) of 0.0002. The substrate had a thickness H while the overall dimension of the substrate was (Length × Width) $A_X \times A_Y$. The radiator of the proposed antenna was embedded on the top side of the substrate, which consisted of a titled W-shaped serpentine structure fed by a microstrip line with a dimension of $F_X \times F_Y$. The backside of the substrate consisted of a partial ground plane of length G_X. A rectangle-shaped slot was etched from a ground plane, and a capacitor was loaded at the center of the slot using two small stubs of thickness g. The simulations were

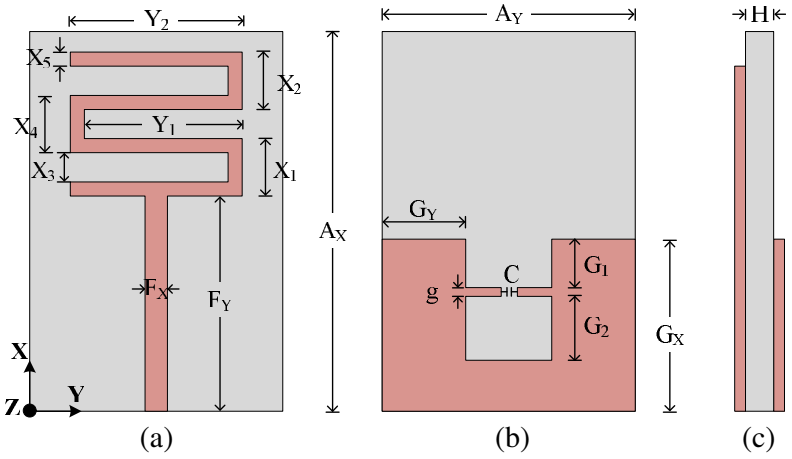

Figure 1. Geometrical configuration of the proposed antenna (a) top-view, (b) back-view, (c) side-view.

carried out using Higher Frequency Structural Simulator (HFSS) while CST Studio Suit was utilized to perform the conformability tests.

The optimized parameters of the proposed antenna are $A_X = 78\,\text{mm}$; $A_Y = 40\,\text{mm}$; $H = 0.254\,\text{mm}$; $G_X = 28\,\text{mm}$; $G_Y = 15\,\text{mm}$; $G_1 = 10\,\text{mm}$; $G_2 = 14\,\text{mm}$; $g = 2\,\text{mm}$; $F_X = 3.5\,\text{mm}$; $F_Y = 44\,\text{mm}$; $X_1 = 14\,\text{mm}$; $X_2 = 14\,\text{mm}$; $X_3 = 5\,\text{mm}$; $X_4 = 14\,\text{mm}$; $X_5 = 4\,\text{mm}$; $Y_1 = 30\,\text{mm}$; $Y_2 = 36\,\text{mm}$; $C = 100\,\text{pF}$.

2.2. Design Methodology

Figure 2 illustrates the various steps involved in designing the proposed antenna and their corresponding return loss. The antenna designing was divided into four major parts:

Step 1. Design an antenna resonating at 2450 MHz.

Step 2. Shift the resonating frequency to a lower band value.

Step 3. Perform impedance matching at the lower resonance.

Step 4. Use capacitor loading to achieve dual band behavior.

At the first step, a simple quarter-wave monopole antenna was designed for the central frequency of 2450 MHz. The length (F_Y) of the transmission line can be estimated using the relation provided in [20]:

$$F_Y = \frac{c}{2f_c\sqrt{\varepsilon_{eff}}} \tag{1}$$

here f_c is the desire central frequency, c the free space speed of light ($\approx 3 \times 10^8\,\text{ms}^{-1}$), and ε_{eff} the effective dielectric constant which can be estimated using the following relation:

$$\varepsilon_{eff} = \frac{\varepsilon_r + 1}{2} \tag{2}$$

here ε_r is the dielectric constant of the substrate. The length and width of the ground plane can also be expressed as the integral part of the wavelength by using the following relation:

$$G_N = \frac{c}{x_n f_c\sqrt{\varepsilon_{eff}}} \tag{3}$$

For length (G_X) of the substrate $x_n \approx 4.5$, and for width (A_Y) of the substrate $x_n \approx 3$. The resultant antenna shows resonance around 2.45 GHz having an $|S_{11}| > -10\,\text{dB}$ impedance bandwidth of 240 MHz ranging 2.37–2.61 MHz, as depicted in Figure 2(b). Next, in Step 2 a serpentine structure was utilized to achieve lower resonance without affecting the overall size of the antenna. Thus, a tilted W-shaped serpentine structure was constructed, where the total effective length of the serpentine can be estimated by [21]:

$$L_T = x_o\frac{c}{f_c\sqrt{\varepsilon_{eff}}} \tag{4}$$

Here L_T is the total effective length of the serpentine, and for the presented antenna it was expressed as $L_T = 4 \times Y_2 + X_1 + X_2 + X_4$, where x_o is the fractional part of the wavelength at the desire frequency and for presented case $x_o \approx 0.55$. Although the resultant antenna showed a resonance at the lower frequency around the 900 MHz, the return loss of the resultant antenna was very low. Thus, to improve the return loss of the antenna Defected Ground Structure (DGS) was utilized. In the third step, a rectangular slot was etched from the center of the ground plane, which resulted in a U-shaped ground plane, as depicted in Figure 2(a). The resultant antenna shows a good impedance matching at the lower frequency of 875 MHz with an impedance bandwidth of 200 MHz ranging from 775–975 MHz. Although the desired lower band of 900 MHz was covered by the antenna, the return loss was still high at 2450 MHz. Thus, to overcome this, a capacitor was loaded in the middle of the slot in the ground plane, as depicted in Figure 2(a). The presence of a capacitor introduces an additional capacitor load, which nullifies the inductive load due to the transmission line and results in higher resonance. The final antenna exhibits a dual-band behavior having resonance around 900 MHz and 2450 MHz with a respective impedance bandwidth of 200 MHz and 570 MHz, as illustrated in Figure 2(b).

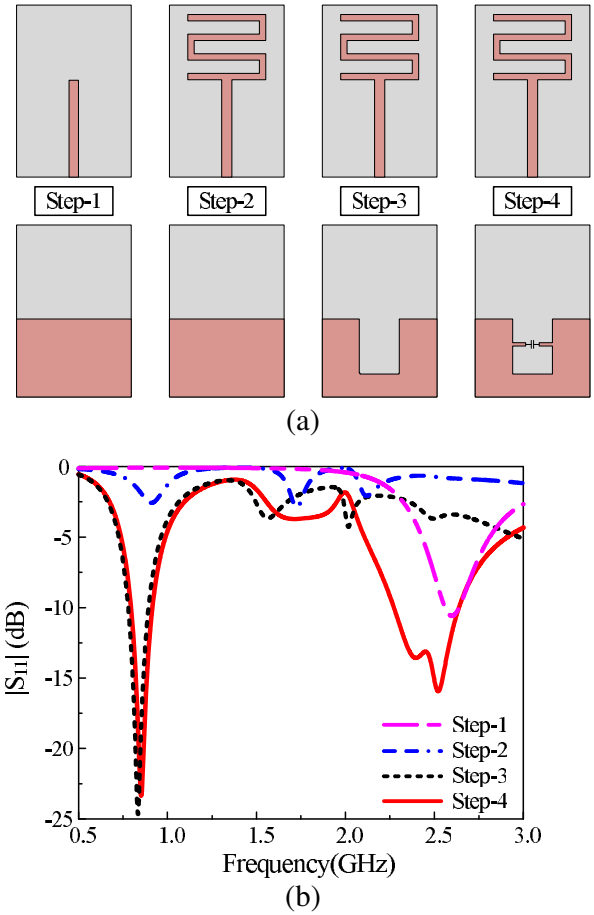

Figure 2. (a) Geometrical configuration of various antennas involve in designing of proposed antenna, (b) return loss comparison between various antennas.

2.3. Equivalent Circuit Model

An equivalent circuit model for the proposed dual band antenna is designed in Advanced Designed System (ADS) software as shown in Figure 3. This circuit is designed for the measurement of input

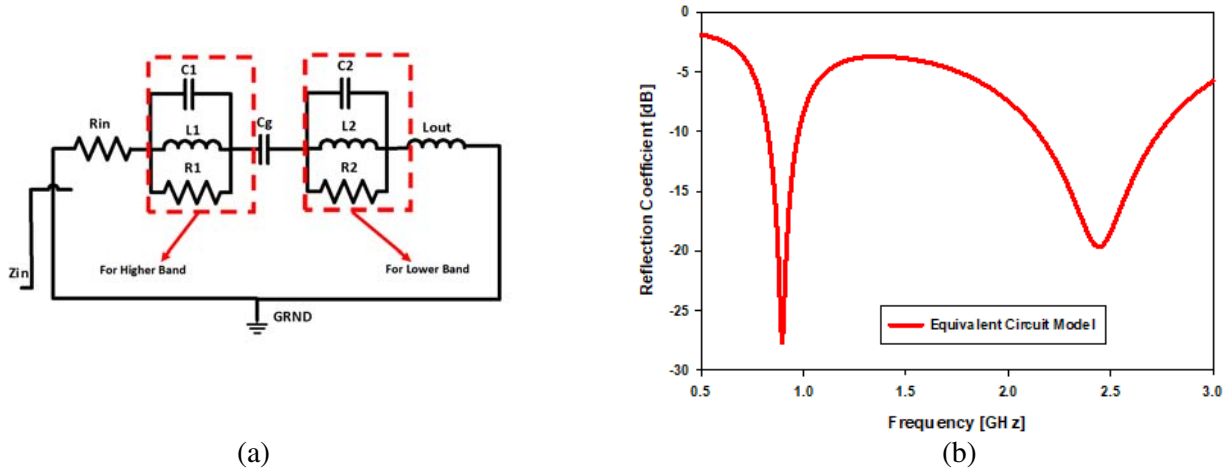

Figure 3. (a) Equivalent circuit of the proposed antenna, (b) simulated results for equivalent circuit.

Table 1. RLC values for equivalent circuit model.

Inductor	Value (nH)	Capacitor	Value (pF)	Resistor	Value (Ω)
$L1$	1.9	$c1$	2.9	Rin	4
$L2$	2.5	$c2$	14.5	$R1$	65
$Lout$	3	cg	100	$R2$	67

impedance matching which can be easily utilized to build an equivalent circuit of dual-band antenna. The circuit model consists of two RLC (resistor-inductor-capacitor) parallel circuit connected in series with a resistor, an inductor, and a capacitor. Their values are given in Table 1. From Figure 3(a), it is clear that both RLC circuits are utilized to achieve dual frequency bands, i.e., 900 MHz and 2450 MHz. The first RLC circuit is connected in series with input resistor (Rin) to achieve high frequency band, i.e., 2450 MHz. The second RLC circuit is connected in series with one inductor ($Lout$) to achieve lower frequency band, i.e., 900 MHz. Both RLC circuits are connected with one ground capacitor (Cg), and it introduces an additional capacitive load, which nullifies the inductive load to improve the resonance frequency. Resistors are used to increase the return loss [dB] to keep it less than −10 dB. Reflection coefficient of the antenna can be tuned by varying the values of the resistors. The simulated reflection coefficients of the proposed design with circuit model is presented in Figure 3(b).

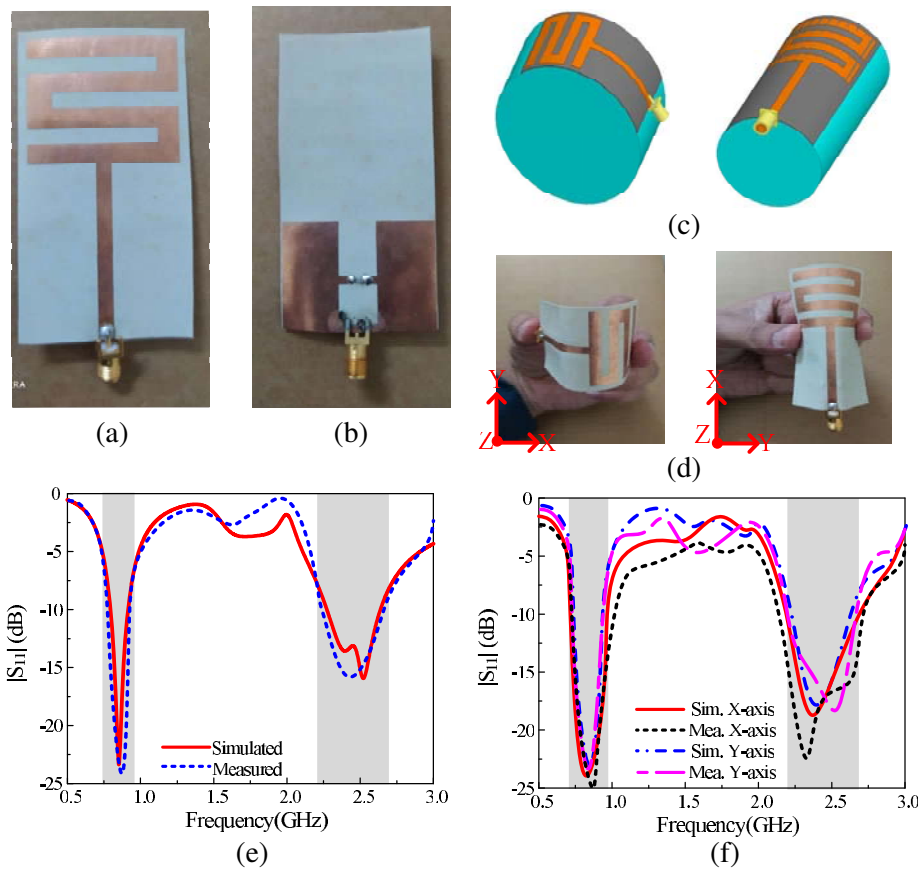

Figure 4. Fabricated antenna prototype (a) top-view, (b) bottom view; Setup for bending analysis (c) simulated, (d) measured; (e) comparison between simulated and measured results, (f) comparison between results under bending condition.

3. RESULTS AND DISCUSSION

3.1. Scattering Parameters

Figure 4 illustrates the fabricated prototype of the antenna under conformal and non-conformable conditions along with the comparison between predicted and measured results. Figures 4(a)–(b) present the top and bottom views of the fabricated prototype used for measurements. A commercially available 50-Ω SMA connector was used for the excitation of the antenna. E5063A ENA Network Analyzer with a frequency range of 500 MHz–18 GHz was used to measure return loss of the antenna. Figure 4(e) presents the comparison between simulated and measured results of the antenna under normal condition, and the antenna shows a good agreement between the two results while exhibiting a wideband of 220 MHz (760–980 MHz) and 570 MHz (2200–2770 MHz) at the resonating frequencies of 900 MHz and 2450 MHz, respectively.

Figure 4(c) depicts the simulation setup for the conformability analysis of the antenna along the X-axis and Y-axis, while Figure 4(d) illustrates the measurements setup for the bending analysis of the proposed dual-band antenna. For both X- and Y-axes, the antenna exhibits a strong agreement between simulated and measured results, as depicted in Figure 4(f). The measured bandwidths of the antenna while it is bent along X-axis are 245 MHz (750–995 MHz) and 720 MHz (2130–2850 MHz), and while it is bent along Y-axis the measured bandwidths are 270 MHz (728–998 MHz) and 585 MHz (2230–2815 MHz) at the resonating frequencies of 900 MHz and 2450 MHz, respectively.

3.2. Radiation Pattern

Figures 5(b)–(c) depict the comparison between simulated and measured radiation patterns at the respective frequencies of 900 MHz and 2450 MHz. It could be observed from Figures 5(b)–(c) that

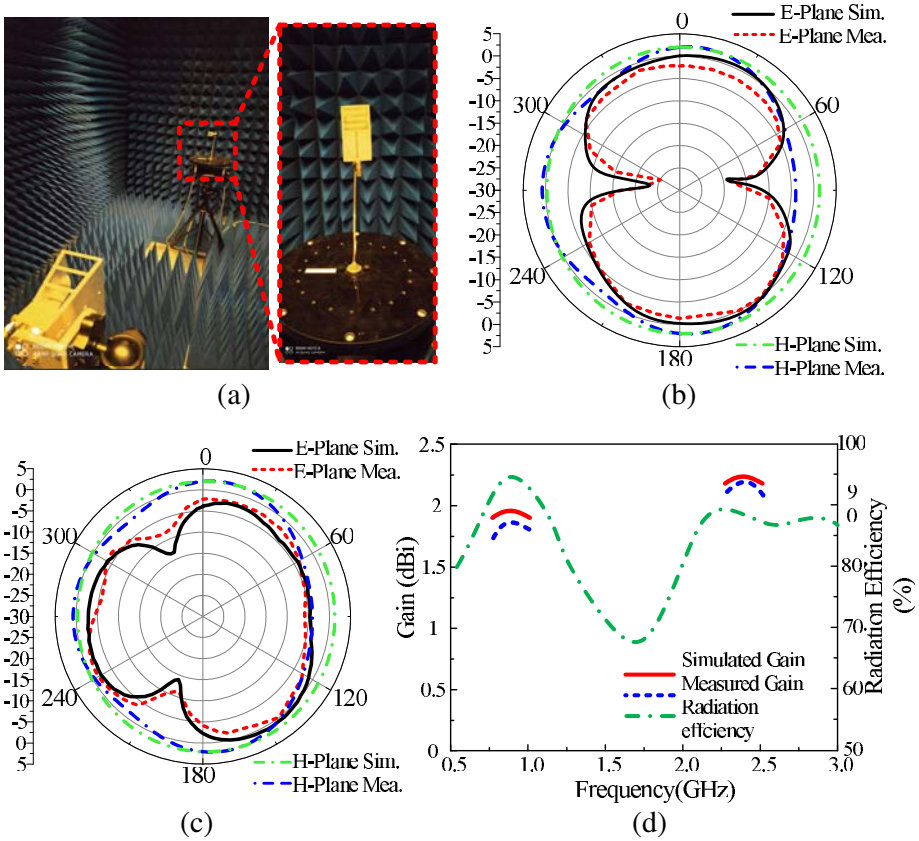

Figure 5. (a) Measurements setup; (b), (c) simulated and measured radiation pattern at 900 MHz and 2450 MHz, respectively; (d) simulated radiation efficiency and measured gain.

the antenna exhibits nearly omnidirectional radiation pattern in principle H-plane ($\theta = 0°$), while a slightly distorted bi-directional radiation pattern was observed in principle E-plane ($\theta = 90°$). The measured radiation pattern results show a strong agreement with the simulated ones, as depicted in Figures 5(b)–(c), indicating the performance stability of the proposed antenna.

3.3. Gain and Efficiency

Figure 5(d) illustrates the comparison between simulated and measured gains of the proposed antenna. At the low passband region, the simulated gain is 1.99 dB while the measured value shows a peak gain of 1.85 dB. On the other hand, the higher passband exhibits a simulated peak gain of 2.27 dB, while the measured value shows a gain of 2.2 dB. The negligible difference between the simulated and measured results is due to fabrication tolerance and random error in the measurement setup. Moreover, the antenna exhibits simulated efficiency $> 85\%$ for both passbands.

3.4. Comparison with State-of-the-Art-Work

Table 2 presents the comparison of the proposed antenna with reported works in literature. It could be observed that the proposed work offers compact size as compared to [9, 10, 13–16], although the antenna presented in [11, 12] has compact size as compared to this work, their work is limited to rigid circuits along with narrow bandwidth. Thus, it can be concluded that the proposed antenna outperforms other related works and becomes a potential candidate for the present and future communication systems.

Table 2. Performance comparison with existing works.

Ref.	Size (mm^2)	Dimension ($\lambda_o \times \lambda_o$)	Impedance Bandwidth (MHz)	Peak Gain (dBi)	Efficiency (%)	Flexibility
[7]	30×25	0.26×0.20	450	2.4	≥ 90	Yes
[8]	100×60	0.30×0.18	200/350	1.6/1.9	N.R	Yes
[9]	115×90	0.35×0.27	580/640	1.25/1.53	N.R	Yes
[10]	15×15	0.13×0.13	30/70	5.34/4.49	N.R	No
[11]	65×46	0.2×0.14	40/70	N.R	N.R	No
[12]	70×80	0.21×0.24	70/800	N.R	N.R	No
[13]	44×48	0.35×0.39	30/40	1.9 / 2.7	N.R	No
[14]	90×100	0.27×0.30	200/70	1.3/2.4	N.R	Yes
[15]	60×60	0.24×0.18	150/250	1.5/2.4	N.R	Yes
This work	78×40	0.23×0.12	220/570	1.85/2.2	93/87	Yes

4. CONCLUSION

In this paper, a compact dual-band flexible antenna was proposed. A simple microstrip antenna was converted into a dual-band antenna by utilizing various techniques including serpentine structures, DGS, and capacitor loading. The antenna consists of a simple geometrical configuration yet covering wide bandwidth of at least 220 MHz ranging 760–980 MHz and 570 MHz ranging 2200–2770 MHz for the respective frequencies of 900 MHz and 2450 MHz. The antenna offers high gain values of 1.85 dBi and 2.2 dBi at the respective frequencies along with simulated efficiency of $> 85\%$. The strong agreement between simulated and measured results as well as conformal and non-conformal results states the performance stability of the antenna. Moreover, a comparison with existing works in the literature shows that the proposed antenna has superior performance and thus becomes a strong candidate for both rigid and flexible devices operating at ISM bands of 900/2450 MHz.

REFERENCES

1. Buckley, J. L., et al., "A dual-ISM-band antenna of small size using a spiral structure with parasitic element," *IEEE Antennas and Wireless Propagation Letters*, Vol. 15, 630–633, 2015.
2. Usluer, M., B. Cetindere, and S. C. Basaran, "Compact implantable antenna design for MICS and ISM band biotelemetry applications," *Willey Microwave and Optical Technology Letters*, Vol. 62, No. 4, 1581–1587, 2020.
3. Naqvi, S. A. and M. S. Khan, "Design of a miniaturized frequency reconfigurable antenna for rectenna in WiMAX and ISM frequency bands," *Willey Microwave and Optical Technology Letters*, Vol. 60, No. 2, 325–330, 2018.
4. Basir, A., A. Bouazizi, M. Zada, A. Iqbal, S. Ullah, and U. Naeem, "A dual-band implantable antenna with wide-band characteristics at MICS and ISM bands," *Willey Microwave and Optical Technology Letters*, Vol. 60, No. 12, 2944–2949, 2018.
5. Hussain, N., W. A. Awan, S. I. Naqvi, A. Ghaffar, A. Zaidi, S. A. Naqvi, and X. J. Li, "A compact flexible frequency reconfigurable antenna for heterogeneous applications," *IEEE Access*, Vol. 8, 173298–173307, 2020.
6. Mohamadzade, B., R. B. Simorangkir, S. Maric, A. Lalbakhsh, K. P. Esselle, and R. M. Hashmi, "Recent developments and state of the art in flexible and conformal reconfigurable antennas," *Electronics*, Vol. 9, No. 9, 1375, 2020.
7. Ghaffar, A., X. J. Li, W. A. Awan, and N. Hussain, "A compact dual-band antenna based on defected ground structure for ISM band applications," *24th International ITG Workshop on Smart Antennas*, 1–2, Hamburg, Germany, February 2020.
8. Awan, W. A., N. Hussain, and T. T. Le, "Ultra-thin flexible fractal antenna for 2.45 GHz application with wideband harmonic rejection," *AEU-International Journal of Electronics and Communications*, Vol. 110, 152851, 2019.
9. Hassan, A., S. Ali, G. Hassan, J. Bae, and C. H. Lee, "Inkjet-printed antenna on thin PET substrate for dual band Wi-Fi communications," *Springer Microsystem Technologies*, Vol. 23, No. 8, 3701–3709, 2017.
10. Ahmed, S., F. A. Tahir, and H. M. Cheema, "A flexible low cost fractal-slot multiband antenna for wireless applications," *IEEE 9th European Conference on Antennas and Propagation (EuCAP)*, 1–4, Lisbon, Portugal, April 2015.
11. Haerinia, M. and S. Noghanian, "A printed wearable dual-band antenna for wireless power transfer," *MDPI Sensors*, Vol. 19, No. 7, 1732, 2019.
12. Masihi, S., M. Panahi, A. K. Bose, D. Maddipatla, A. J. Hanson, B. B. Narakathu, and M. Z. Atashbar, "Rapid prototyping of a tunable and compact microstrip antenna by laser machining flexible copper tape," *IEEE International Conference on Flexible and Printable Sensors and Systems (FLEPS)*, 1–3, Glasgow, UK, July 2019.
13. Zhao, Y., Y. Lv, T. Si, G. Du, M. Li, and Y. Yu, "Design of a miniaturized dual-frequency monopole antenna for applications in IoT," *IEEE 6th International Conference on Systems and Informatics (ICSAI)*, 1051–1055, Shanghai, China, November 2019.
14. Forouzannezhad, P., A. Jafargholi, and A. Jahanbakhshi, "Multiband compact antenna for near-field and far-field RFID and wireless portable applications," *IET Microwaves, Antennas and Propagation*, Vol. 11, No. 4, 525–541, 2016.
15. Kim, S. and M. M. Tentzeris, "Parylene coated waterproof washable inkjet-printed dual-band antenna on paper substrate," *International Journal of Microwave and Wireless Technologies*, Vol. 10, No. 7, 814–818, 2018.
16. Khajeh-Khalili, F., F. Haghshenas, and A. Shahriari, "Wearable dual-band antenna with harmonic suppression for application in medical communication systems," *AEU-International Journal of Electronics and Communications*, Vol. 126, 153396, 2020.
17. Iqbal, A., I. B. Mabrouk, and M. Nedil, "Compact siw-based self-quadruplexing antenna for wearable transceivers," *IEEE Antennas and Wireless Propagation Letters*, Vol. 20, No. 1, 118–122, 2020.

18. Elfergani, I., A. Iqbal, C. Zebiri, A. Basir, J. Rodriguez, M. Sajedin, and S. Ullah, "Low-profile and closely spaced four-element MIMO antenna for wireless body area networks," *Electronics*, Vol. 9, No. 2, 258, 2020.
19. Iqbal, A., A. J. Alazemi, and N. K. Mallat, "Slot-DRA-based independent dual-band hybrid antenna for wearable biomedical devices," *IEEE Access*, Vol. 7, 184029–184037, 2019.
20. Balanis, C. A., *Antenna Theory: Analysis and Design*, John Wiley & Sons, New York, 2015.
21. Awan, W. A., N. Hussain, S. A. Naqvi, A. Iqbal, R. Striker, D. Mitra, and B. D. Braaten, "A miniaturized wideband and multi-band on-demand reconfigurable antenna for compact and portable devices," *AEU-International Journal of Electronics and Communications*, Vol. 122, 153266, 2020.